

Semi-Experimental Equilibrium (r_e^{SE}) and Theoretical Structures of Pyridazine ($o\text{-C}_4\text{H}_4\text{N}_2$)

Andrew N. Owen, Maria A. Zdanovskaia, Brian J. Esselman, John F. Stanton, R. Claude Woods,* and Robert J. McMahon*



Cite This: *J. Phys. Chem. A* 2021, 125, 7976–7987



Read Online

ACCESS |



Metrics & More

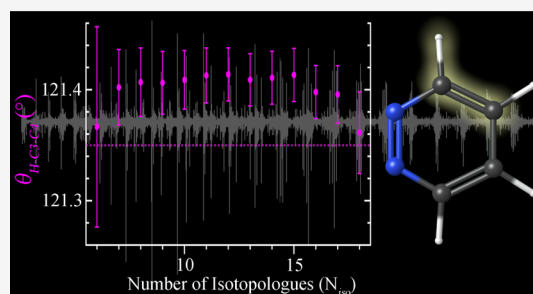


Article Recommendations



Supporting Information

ABSTRACT: A semi-experimental equilibrium structure (r_e^{SE}) of pyridazine ($o\text{-C}_4\text{H}_4\text{N}_2$) has been determined using the rotational spectra of 18 isotopologues. Spectroscopic constants of four isotopologues are reported for the first time (measured from 235 to 360 GHz), while spectroscopic constants for previously reported isotopologues are improved by extending the frequency coverage (measured from 130 to 375 GHz). The experimental values of the ground-state rotational constants (A_0 , B_0 , and C_0) from each isotopologue were converted to determinable constants (A_0'' , B_0'' , and C_0''), which were then corrected for the effects of vibration–rotation interactions and electron-mass distributions using CCSD(T)/cc-pCVTZ calculations. The resultant r_e^{SE} for pyridazine determines bond distances to within 0.001 Å and bond angles within 0.04°, a reduction in the statistical uncertainties by at least a factor of two relative to the previously reported r_e^{SE} . The improvement in precision appears to be largely due to the use of higher-level theoretical calculations of the vibration–rotation and electron-mass effects, though the incorporation of the newly measured isotopologues ($[4\text{-}^2\text{H}, 4\text{-}^{13}\text{C}]$ -, $[4\text{-}^2\text{H}, 5\text{-}^{13}\text{C}]$ -, $[4\text{-}^2\text{H}, 6\text{-}^{13}\text{C}]$ -, and $[4,5\text{-}^2\text{H}, 4\text{-}^{13}\text{C}]$ -pyridazine) is partially responsible for the improved determination of the hydrogen-containing bond angles. The computed equilibrium structure (r_e) (CCSD(T)/cc-pCVSZ) and a “best theoretical estimate” of the equilibrium structure (r_e) both agree with the updated r_e^{SE} structure within the statistical experimental uncertainty (2σ) of each structural parameter.



INTRODUCTION

Pyridazine ($o\text{-C}_4\text{H}_4\text{N}_2$, C_{2v} , $\mu = 4.22$ D, Figure 1) is an aromatic heterocycle in which adjacent C–H units of benzene are replaced by nitrogen atoms (Figure 2). As a prototypical aromatic heterocycle,^{1,2} it is a species of astrochemical relevance.^{3–5} Benzene has been detected in the interstellar medium by infrared spectroscopy,⁶ but it cannot be observed by radioastronomy because it lacks a permanent dipole moment. Aromatic compounds that are polar by virtue of inherent structural factors,^{7–9} heteroatom substitution,^{3–5} or

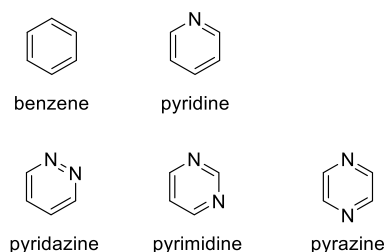


Figure 2. Benzene and nitrogen-containing analogues.

polar substituents^{10–12} have been important targets for astronomical detection (Figure 2). The recent detections of polar aromatic compounds by radioastronomy (benzonitrile¹³ and cyanonaphthalenes¹⁴) represent dramatic breakthroughs in astrochemistry and will undoubtedly inspire new searches for aromatic heterocycles.

Received: July 11, 2021

Revised: August 14, 2021

Published: September 3, 2021

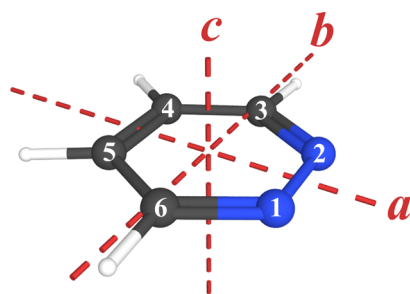


Figure 1. Pyridazine ($o\text{-C}_4\text{H}_4\text{N}_2$, C_{2v} , $\mu = 4.22$ D, $\kappa = 0.824$) with principal axes and atom numbering.

Some time ago, Werner *et al.*¹⁵ measured the rotational spectrum of pyridazine and its singly heavy-atom-substituted isotopologues from 9 to 33 GHz and obtained a partial substitution structure (r_s). In that first structure determination, parameters involving hydrogen atoms were held constant because rotational constants from deuterium-containing isotopologues were not available. López *et al.*¹⁶ reported improved values for the rotational constants with precise Fourier-transform microwave (FT-MW) measurements of hyperfine-resolved transitions. Several years later, our group measured the spectrum of pyridazine at a higher frequency (235–360 GHz), reporting spectroscopic constants for the ground state and six lowest-energy vibrationally excited states of the normal isotopologue.⁵ These measurements enabled the first direct comparison of the experimental and predicted [CCSD(T)] vibration–rotation interaction constants for an organic molecule of this size, demonstrating good agreement between the two. Building on the synergy of experiment and theory, the investigation was expanded to include a semi-experimental structure (r_e^{SE}) determination for pyridazine. Spectroscopic constants for a total of 14 isotopologues were measured, including the normal isotopologue, 3 singly substituted heavy-atom isotopologues detectable at natural abundance, and 10 deuterium-substituted isotopologues from enriched samples. Using CCSD(T) corrections to the rotational constants to account for the vibration–rotation interaction and electron-mass distribution, a complete semi-experimental equilibrium structure (r_e^{SE}) of pyridazine that included hydrogen-containing structural parameters was determined for the first time. That study determined a highly precise r_e^{SE} of pyridazine with statistical uncertainties (2σ) on the order of 0.003 Å for bond distances and 0.1° for bond angles.

The semi-experimental equilibrium structure of pyridazine⁵ represented a significant advance in the gas-phase structure determination of organic molecules. Since then, however, a new standard for precision and accuracy has been achieved for r_e^{SE} structure determinations, in general, and for aromatic heterocycles, in particular.^{17–19} In a striking result, each of the structural parameters of pyrimidine (the *meta*-dinitrogen analogue of pyridazine; Figure 2) predicted by the best available theoretical methods agree with those determined in the semi-experimental equilibrium (r_e^{SE}) structure to within the 2σ statistical uncertainties of the latter.¹⁷ The current work aims to incorporate new spectroscopic data, improve the computational treatment, and raise the precision of the r_e^{SE} structure of pyridazine to that same standard. The previous observation, measurement, and least-squares fitting of the [4-²H, 3-¹³C]-isotopologue of pyridazine implied that the spectra of the [4-²H, 4-¹³C]-, [4-²H, 5-¹³C]-, and [4-²H, 6-¹³C]-isotopologues²⁰ should also be observable in the existing spectrum due to sharing the same natural ¹³C abundance, without the need for additional synthesis or spectroscopy. Indeed, we identified transitions for these new species and included their spectroscopic constants in the current structure determination. Rotational constants for the normal and singly heavy-atom substituted isotopologues were improved by extending frequency coverage down to 130 GHz and up to 375 GHz. The use of a larger, all-electron basis set (cc-pCVTZ) improved the quality of the vibration–rotation corrections used to determine the equilibrium rotational constants and consequent moments of inertia. Finally, the electron-mass correction was improved by incorporating

corrections specific to each isotopologue. Such an improved r_e^{SE} structure for pyridazine provides an opportunity to test the generality of the close agreement between the experiment and theory observed for pyrimidine.¹⁷

In the current investigation of the r_e^{SE} of pyridazine, we also explore the effect of adding more isotopologues to the data set beyond those minimally needed to determine the structure. Traditionally, the minimal set of isotopologues required to obtain a substitution structure (r_s) includes the normal and all singly substituted isotopologues.^{21,22} Although spectroscopic data from additional, multiply substituted isotopologues provides further constraints on atom positions and thereby improves the precision and accuracy of the structure, such an approach is not typically employed. The trade-off for this improvement is the increased experimental effort needed to acquire spectroscopic data for additional isotopologues, particularly if they are not observable at natural abundance and require chemical synthesis/isotopic enrichment. Therefore, to inform our choice of the number of additional isotopologues to include in structure determination, we systematically examine the effect of including isotopologues beyond the minimal set on the r_e^{SE} structure.

EXPERIMENTAL METHODS

The rotational spectrum of pyridazine, previously reported in the frequency range of 235–360 GHz,⁵ was measured from 130 to 375 GHz using a rotational spectrometer described elsewhere.^{5,10,23} A commercial sample of pyridazine was used without purification at a sample pressure of 0.5–7 mTorr at room temperature using a continuous flow. The spectral ranges were combined into a single broadband spectrum and each species was least-squares fit to a distorted-rotor Hamiltonian using Assignment and Analysis of Broadband Spectra (AABS) software.^{24,25} PLANM and AC programs were used for data analysis.²⁶ In our least-squares fits, we assume a uniform frequency measurement uncertainty of 50 kHz. All deuterium-enriched pyridazine spectra were collected previously from samples synthesized by base-catalyzed hydrogen/deuterium exchange.⁵

COMPUTATIONAL METHODS

A development version of CFOUR²⁷ was employed to conduct all *ab initio* calculations, which consisted of geometry optimizations, anharmonic second-order vibrational perturbation theory (VPT2), and magnetic property calculations at the CCSD(T) level of theory using the all-electron cc-pCVTZ basis. Isotopologue-dependent corrections to the rotational constants included vibration–rotation interaction constants from the VPT2 calculations and electron-mass corrections from magnetic property calculations. Output files of these calculations are provided in the [Supporting Information](#).

We calculated a “best theoretical estimate” (BTE) equilibrium structure for pyridazine using the methodology employed in previous studies of pyrimidine,¹⁷ thiophene,¹⁸ and thiazole.¹⁹ The structure computed using a CCSD(T)/cc-pCVSZ optimization is corrected to account for the following limitations associated with the quantum mechanical treatment employed:

1. Residual basis set effects, eq 1, by means of a complete basis set extrapolation^{28,29} using the results of CCSD(T)/cc-pCVXZ ($X = T, Q,$ and 5) calculations in comparison to the quintuple zeta optimization.

$$\Delta R (\text{basis}) = R(\infty) - R(\text{CCSD(T)/cc-pCVSZ}) \quad (1)$$

2. Residual electron correlation effects, eq 2, by use of CCSDT(Q)³⁰ in comparison to a CCSD(T) optimization.

$$\Delta R (\text{corr}) = R(\text{CCSDT(Q)/cc-pVDZ}) - R(\text{CCSD(T)/cc-pVDZ}) \quad (2)$$

3. Scalar relativistic effects, eq 3, by use of the X2C-1e variant of the coupled-cluster theory^{31–33} in comparison to a traditional optimization (NR).

$$\Delta R (\text{rel}) = R(\text{CCSD(T)/cc-pCVTZ})_{\text{SFX2C-1e}} - R(\text{CCSD(T)/cc-pCVTZ})_{\text{NR}} \quad (3)$$

4. Effect of the Born–Oppenheimer approximation, eq 4, by use of the diagonal Born–Oppenheimer correction (DBOC)^{34,35} in comparison to a traditional optimization (NR).

$$\Delta R (\text{DBOC}) = R(\text{SCF/cc-pCVTZ})_{\text{DBOC}} - R(\text{SCF/cc-pCVTZ})_{\text{NR}} \quad (4)$$

5. The correction to the CCSD(T)/cc-pCVSZ optimization necessary to obtain the BTE is then given by the summation of the above corrections for each parameter, as shown in eq 5.

$$\Delta R (\text{best}) = \Delta R (\text{basis}) + \Delta R (\text{corr}) + \Delta R (\text{rel}) + \Delta R (\text{DBOC}) \quad (5)$$

r_e^{SE} Structure Determination. The semi-experimental equilibrium structural parameters (r_e^{SE}) of pyridazine were determined from the equilibrium moments of inertia by least-squares fitting, as described for previous structure determinations.^{5,17–19,23} In total, 18 isotopologues yield 36 independent moments of inertia, which produce a highly redundant determination of the 9 independent structural parameters of pyridazine (point group symmetry C_{2v}). In this work, all 3 moments of inertia for all 18 isotopologues were used with equal weighting. To generate constants free of centrifugal distortion and the impact of the choice of an A- or S-reduced Hamiltonian, the rotational constants (B_0^x) determined in each least-squares fit were converted to determinable constants (B_0^y) using eqs S1–S6³⁶ in the **Supporting Information**. For each of the isotopologues presented in this work, differences in the determinable constants from the A and S reductions were quite small (Table S2), demonstrating that both the A- and S-reduced Hamiltonians produce physically meaningful spectroscopic constants. This gives us high confidence that the average determinable rotational constants are largely free of the effects of centrifugal distortion. The computed vibration–rotation interaction and electron-mass corrections were combined with the averaged determinable constants to obtain the semi-experimental equilibrium constants (B_e^x) using eq S7.^{17–19,23} These equilibrium constants, after conversion to the corresponding moments of inertia, were used by the *xrefit* module of CFOUR to determine the r_e^{SE} structural parameters *via* a nonlinear least-squares fit, using the Levenberg–Marquardt algorithm.

The high accuracy and precision of our recent semi-experimental structure determinations derive, in part, from the inclusion of a large number of multiply substituted

isotopologues in the data sets.^{5,17–19,23} This approach contrasts with the Kraitchman analysis for structure determination (r_s substitution structure)^{21,22} and other implementations of the semi-experimental structure determination (r_e^{SE})^{37,38} that commonly rely on single-atom isotopic substitution. While single-atom isotopic substitution is sufficient for determining a molecular structure, the data set of singly substituted isotopologues represents the smallest set that is sufficient to do so.³⁹ Herein, we refer to a data set consisting of the normal isotopologue and singly substituted isotopologues as the “minimal data set”. Since the data sets for our structural determinations substantially exceed the “minimal data set”, there are opportunities to develop new methods for analyzing and interpreting data.

To assess the impact of the number of isotopologues (N_{iso}) included in a data set used for an r_e^{SE} structure determination, one could simply compare the r_e^{SE} structure obtained using a minimal set of isotopologues to the r_e^{SE} structure obtained using all of the available isotopologues. This comparison, however, does not provide information about how the r_e^{SE} structure changes as a function of N_{iso} or how the incorporation of additional isotopologues impacts the structure. A more informative approach to assess the impact of the number of isotopologues is to determine the r_e^{SE} structural parameters using the minimal set, then sequentially add each isotopologue to the data set, and observe how the r_e^{SE} structural parameters and their statistical uncertainties change. Because the r_e^{SE} structure is a state function of the moments of inertia with respect to the isotopologues in the data set, the order in which the isotopologues are added has no effect on the final r_e^{SE} structure but does determine the intermediate r_e^{SE} structures that are generated. Determining each intermediate r_e^{SE} structure for every permutation of the addition of all isotopologues would be a rigorous approach, but it is not practical. Not only would it be cumbersome to obtain such an r_e^{SE} analysis,⁴⁰ it is not clear how one would interpret the results. Thus, the analysis method requires a different procedure for selecting which isotopologue should be added to the working set of isotopologues.

We employed an approach where the isotopologue data set is sequentially expanded to include the isotopologue whose inclusion results in the greatest reduction of the statistical uncertainties of the r_e^{SE} parameters. This criterion enables the analysis to probe the change in the r_e^{SE} structure *via* the addition of a single isotopologue. If an isotopologue provides structural information consistent with that already in the data set, adding that isotopologue should have the impact of reducing the overall statistical uncertainty by providing redundant information. If an isotopologue provides structural information that is not consistent with the rest of the data set (due to poor determination of its spectroscopic constants, providing structural information counter to that provided in the current data set, high error in the atomic position due to the location of principal axes, etc.), adding that isotopologue may result in r_e^{SE} structural parameters with larger statistical uncertainty. Because all isotopologues will eventually be added to the r_e^{SE} , the isotopologues that are not consistent with the rest of the data set will be represented by a characteristic increase in the statistical uncertainty at the end of the routine (*vide infra*).

In this work, we present the details of a new script that we developed for examining the impact of each isotopologue on the r_e^{SE} structure. The script has been dubbed *xrefiteration*

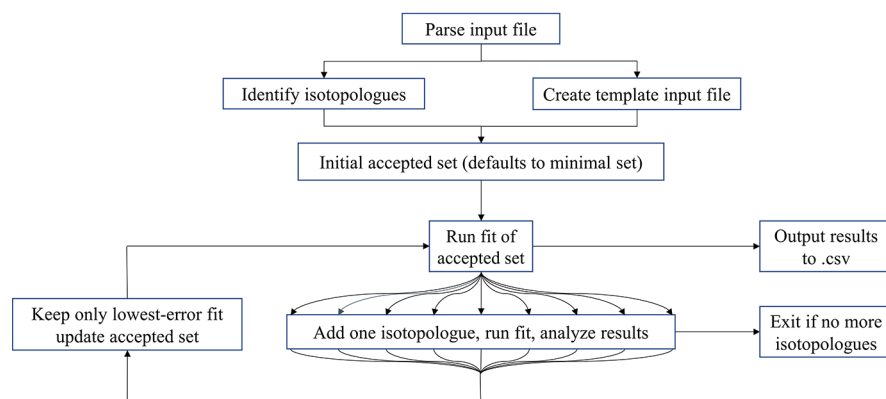


Figure 3. Flow chart depicting the *xrefit* iteration algorithm.

Table 1. Experimental Spectroscopic Constants for the Normal and Newly Analyzed Isotopologues of Pyridazine (S-Reduced Hamiltonian, III^F Representation)^a

	<i>o</i> -C ₄ H ₄ N ₂	[4- ² H, 4- ¹³ C]	[4- ² H, 5- ¹³ C]	[4- ² H, 6- ¹³ C]	[4,5- ² H, 4- ¹³ C]
<i>A</i> ₀ (MHz)	6242.951362 (86)	6189.054 (15)	6116.7348 (36)	6081.1083 (34)	5973.7512 (35)
<i>B</i> ₀ (MHz)	5961.093204 (82)	5486.810 (13)	5542.2127 (38)	5580.9717 (37)	5307.9449 (29)
<i>C</i> ₀ (MHz)	3048.714734 (98)	2907.82583 (28)	2907.08047 (28)	2909.57519 (33)	2810.09773 (33)
<i>D</i> _{<i>J</i>} (kHz)	1.474194 (61)	1.3139 (37)	1.31111 (40)	1.31399 (39)	1.19361 (52)
<i>D</i> _{<i>JK</i>} (kHz)	-2.449536 (27)	-2.1633 (48)	-2.16548 (87)	-2.17166 (88)	-1.9646 (11)
<i>D</i> _{<i>K</i>} (kHz)	1.101309 (32)	0.9628 (12)	0.96739 (46)	0.97055 (47)	0.87505 (55)
<i>d</i> ₁ (kHz)	-0.015544 (14)	-0.070 (12)	[-0.0582741]	[-0.0588716]	[-0.0585689]
<i>d</i> ₂ (kHz)	0.0272053 (93)	[-0.0108873]	[0.0142048]	[-0.0118571]	[0.0295905]
<i>H</i> _{<i>J</i>} (Hz)	0.000601 (13)	[0.0005306]	[0.000589]	[0.0005284]	[0.0005381]
<i>H</i> _{<i>JK</i>} (Hz)	-0.0026963 (33)	[-0.0019865]	[-0.0023442]	[-0.001983]	[-0.0022084]
<i>H</i> _{<i>KJ</i>} (Hz)	0.0033337 (64)	[0.0024955]	[0.0027966]	[0.0025002]	[0.002551]
<i>H</i> _{<i>K</i>} (Hz)	-0.0012713 (67)	[-0.0010395]	[-0.0010414]	[-0.0010455]	[-0.0008804]
<i>h</i> ₁ (Hz)	[-0.000008]	[0.0000388]	[0.000029]	[0.000035]	[0.0000212]
<i>h</i> ₂ (Hz)	[-0.0000919]	[0.0000326]	[-0.0000346]	[0.0000364]	[-0.0000798]
<i>h</i> ₃ (Hz)	-0.0000662 (75)	[0.0000218]	[0.000003]	[0.0000249]	[-0.0000149]
<i>Δ</i> ₁ (μÅ ²) ^b	0.036367 (6)	0.03472 (30)	0.034598 (81)	0.034775 (78)	0.032180 (75)
<i>N</i> _{lines} ^c	2560 ^d	254	226	219	196
<i>σ</i> _{fit} (MHz)	0.035	0.041	0.040	0.041	0.042

^aValues in square brackets held constant at the computed value [CCSD(T)/cc-pCVTZ] in the least-squares fit. ^bInertial defect, $\Delta_1 = I_c - I_a - I_b$, calculated using PLANM from the *B*₀ constants. ^cNumber of independent transition frequencies. ^dIncludes 82 independent transitions from ref 15.

(because it iteratively utilizes the *xrefit* module of CFOUR) and has been briefly described in two previous works.^{18,19} It is implemented as a bash shell script, which performs the following algorithm (depicted in Figure 3):

1. For the “accepted set” of isotopologues, execute *xrefit* to obtain an initial r_e^{SE} structure. The initial accepted set can be user-defined, but defaults to the “minimal set” as identified by assuming that the first isotopologue in the input file is the normal isotopologue and identifying all isotopologues that differ by single isotopic substitution.
2. For each isotopologue that is not part of the accepted set, execute *xrefit* to obtain an r_e^{SE} structure using the accepted set of isotopologues plus that additional isotopologue.
3. Of the resulting r_e^{SE} structures obtained in step 2, the additional isotopologue that resulted in the lowest statistical uncertainties of the structural parameters is added to the accepted set of isotopologues. To obtain a single metric by which to evaluate the total statistical uncertainty, we calculated the relative (and thus dimensionless) uncertainties of the bond distances (eq

6), angles (eq 7), and dihedral angles (eq 8), and combined the results to give the total relative statistical uncertainty of the r_e^{SE} structure (δr_e^{SE}) in eq 9.

$$\delta r_e^{\text{SE}} (\text{bonds}) = \sqrt{\sum_i \left(\frac{2\sigma_{\text{fit}}(R_i)}{R_i} \right)^2} \quad (6)$$

$$\delta r_e^{\text{SE}} (\text{angles}) = \sqrt{\sum_i \left(\frac{2\sigma_{\text{fit}}(\theta_i)}{\theta_i} \right)^2} \quad (7)$$

$$\delta r_e^{\text{SE}} (\text{dihedrals}) = \sqrt{\sum_i \left(\frac{2\sigma_{\text{fit}}(\phi_i)}{\phi_i} \right)^2} \quad (8)$$

$$\delta r_e^{\text{SE}} = \sqrt{[\delta r_e^{\text{SE}} (\text{bonds})]^2 + [\delta r_e^{\text{SE}} (\text{angles})]^2 + [\delta r_e^{\text{SE}} (\text{dihedrals})]^2} \quad (9)$$

4. Repeat steps 2 and 3 until all isotopologues have been incorporated into the accepted set, at which point a final r_e^{SE} structure is calculated by executing *xrefit*.

Table 2. Inertial Defects (Δ_i) of Pyridazine Isotopologues from Various Determinations of the Moments of Inertia

isotopologue	pyridazine (2013) ⁵			pyridazine (current work)		
	$\Delta_{i,0}$ ($\mu\text{\AA}^2$)	$\Delta_{i,e}$ ($\mu\text{\AA}^2$) ^a	$\Delta_{i,e}$ ($\mu\text{\AA}^2$) ^b	$\Delta_{i,0}$ ($\mu\text{\AA}^2$)	$\Delta_{i,e}$ ($\mu\text{\AA}^2$) ^c	$\Delta_{i,e}$ ($\mu\text{\AA}^2$) ^d
Normal	0.03641	-0.01200	0.00081	0.03622	-0.01414	-0.00095
[3- ¹³ C]	0.03702	-0.01193	0.00112	0.03681	-0.01410	-0.00090
[4- ¹³ C]	0.03706	-0.01198	0.00116	0.03684	-0.01414	-0.00095
[1- ¹⁵ N]	0.03686	-0.01206	0.00106	0.03671	-0.01414	-0.00095
[3- ² H]	0.03367	-0.01235	0.00133	0.03356	-0.01427	-0.00108
[4- ² H]	0.03406	-0.01228	0.00160	0.03391	-0.01428	-0.00108
[3,4- ² H]	0.03138	-0.01278	0.00195	0.03124	-0.01452	-0.00132
[3,5- ² H]	0.03143	-0.01287	0.00191	0.03132	-0.01455	-0.00135
[3,6- ² H]	0.03072	-0.01250	0.00224	0.03061	-0.01437	-0.00118
[4,5- ² H]	0.03185	-0.01206	0.00283	0.03169	-0.01417	-0.00097
[4- ² H, 3- ¹³ C]	0.03498	-0.01194	0.00218	0.03441	-0.01433	-0.00114
[4- ² H, 4- ¹³ C]				0.03456	-0.01416	-0.00097
[4- ² H, 5- ¹³ C]				0.03450	-0.01419	-0.00099
[4- ² H, 6- ¹³ C]				0.03462	-0.01420	-0.00100
[3,4,5- ² H]	0.02916	-0.01224	0.00351	0.02899	-0.01428	-0.00108
[3,4,6- ² H]	0.02852	-0.01283	0.00295	0.02836	-0.01454	-0.00134
[3,4,5,6- ² H]	0.02625	-0.01234	0.00440	0.02606	-0.01434	-0.00114
[4,5- ² H, 4- ¹³ C]				0.03209	-0.01427	-0.00107
average (\bar{x})	0.03281	-0.01230	0.00207	0.03292	-0.01428	-0.00108
std. dev. (s)	0.00347	0.00033	0.00104	0.00310	0.00014	0.00014

^aVibration-rotation interaction corrections only [CCSD(T)/ANO0]. ^bVibration-rotation interaction and electron-mass corrections [CCSD(T)/ANO0]. ^cVibration-rotation interaction corrections only [CCSD(T)/cc-pCVTZ]. ^dVibration-rotation interaction and electron-mass corrections [CCSD(T)/cc-pCVTZ].

The routine collects various components of the r_e^{SE} calculations it has performed and provides a summary output file (.csv) for analysis. The script, example input and output files, and a more detailed explanation of the routine and its options are included in the Supporting Information. Also included in the Supporting Information is a standalone .html report of the *xrefiteration* analysis for viewing convenience, along with the code used to generate the .html report using the results of the *xrefiteration* script.

RESULTS AND DISCUSSION

Analysis of Rotational Spectra. The rotational spectrum of the main isotopologue of pyridazine has been described previously⁵ and those of its isotopologues are similar in nature. The expanded frequency coverage (130–375 GHz) in the current investigation resulted in a substantial increase in the number of transitions measured for the normal and singly substituted heavy-atom isotopologues. Even though new spectra were not collected for the deuterium-enriched isotopologues, all rotational spectra were re-examined to identify additional transitions for previously measured isotopologues. Additionally, using improved predictions of their spectroscopic constants, four previously unreported isotopologues were identified: [4-²H, 4-¹³C], [4-²H, 5-¹³C], [4-²H, 6-¹³C], and [4,5-²H, 4-¹³C].²⁰ A portion of the experimental spectrum of one of the deuterium-enriched pyridazine samples is provided in Figure 4, featuring visible $^aR_{0,1}$ bands of two newly found isotopologues: [4-²H, 4-¹³C] and [4-²H, 5-¹³C]. The figure provides some insights into why these species were difficult to identify, previously, and why improved initial predictions were needed. Their transition intensities are sufficiently low that even the most intense transitions are only three to four times the spectral confusion limit. This situation is particularly problematic in spectra such as these, which include many isotopologues, each with

corresponding low-lying vibrationally excited states. The identification of the very low-intensity isotopologues was enabled by the updated structure determination, which improved the predictions of the rotational constants of the additional isotopologues.

Updated spectroscopic constants and data distribution plots demonstrating the breadth of quantum numbers analyzed are provided for all isotopologues in the Supporting Information. The updated spectroscopic constants (S-reduced Hamiltonian, III^r representation) for the normal isotopologue and the newly analyzed isotopologues are presented in Table 1. In the least-squares fit of the normal isotopologue, two sextic distortion constants had to be held constant at their theoretical values. Due to the very low intensities of the newly analyzed species in the rotational spectra, the number of observed transitions for each new isotopologue is modest. As a result, all of the sextic distortion constants and at least one quartic distortion constant for each new isotopologue had to be held constant at their predicted values. Nevertheless, the constants that were able to be determined are fairly similar between the various species and appear to be physically meaningful values.

Semi-Experimental Equilibrium (r_e^{SE}) Structure of Pyridazine. Improvement in the Precision and Accuracy of Rotational Constants and Moments of Inertia. For a planar molecule such as pyridazine, an indication of the quality of the computational corrections that are applied to the experimentally determined rotational constants is how close the resultant inertial defect (Δ_i) is to zero. Uncorrected experimental rotational constants (B_0^x) produce a non-zero inertial defect ($\Delta_{i,0}$) due to the effects of vibration-rotation interactions and the distribution of electron mass. By correcting the rotational constants for these effects, the magnitude of the inertial defect is decreased, ultimately vanishing in the limit that the applied corrections are exact. Previously, CCSD(T)/ANO0 vibration-rotation interaction

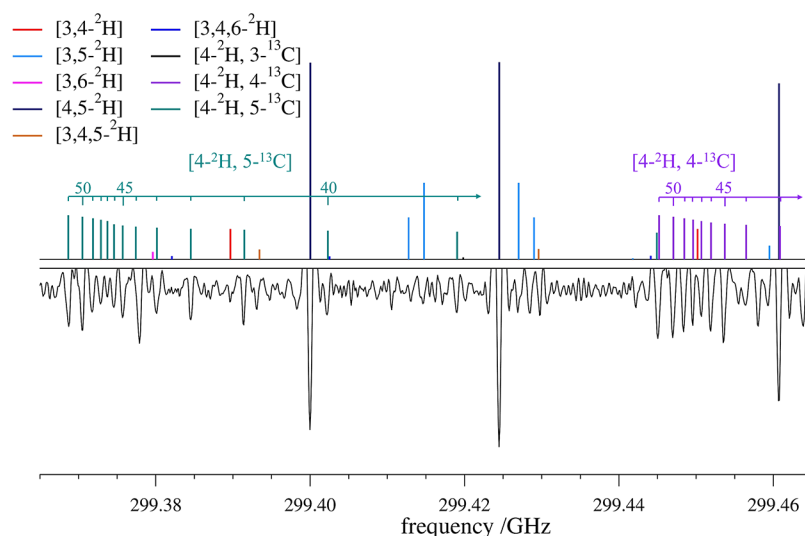


Figure 4. Rotational spectrum of deuterium-enriched pyridazine sample from 299.365 to 299.465 GHz (bottom) and stick spectra of several deuteriated isotopologues (top). The upper state J (i.e., $J'' + 1$) values are marked for the two newly found isotopologues in their corresponding colors. Some transitions belonging to other isotopologues and their vibrational satellites are also visible in the spectrum.

Table 3. Structural Parameters of Pyridazine

parameter	experimental				computational	
	r_e^{SE} (2013) ^a CCSD(T)/ANO0	r_e^{SE} CCSD(T)/cc-pCVTZ			CCSD(T) BTE ^b	CCSD(T)/cc-pCVSZ
		minimal data set	full data set excluding [3,4- ² H]	full data set		
$R_{\text{C3-H}}$ (Å)	1.08104 (54)	1.08088 (20)	1.08093 (15)	1.08088 (23)	1.08108	1.08097
$R_{\text{C4-H}}$ (Å)	1.08021 (74)	1.07992 (22)	1.07989 (16)	1.08000 (24)	1.07995	1.07988
$R_{\text{C4-C5}}$ (Å)	1.3761 (33)	1.37673 (88)	1.37676 (63)	1.37675 (95)	1.37638	1.37656
$R_{\text{C3-C4}}$ (Å)	1.3938 (24)	1.39352 (72)	1.39348 (50)	1.39338 (75)	1.39395	1.39353
$R_{\text{N2-C3}}$ (Å)	1.3302 (24)	1.33085 (70)	1.33082 (53)	1.33093 (79)	1.33091	1.33074
$R_{\text{N1-N2}}$ (Å)		1.33328 (82) ^c	1.33341 (77) ^c	1.33336 (116) ^c	1.33377	1.33215
$\theta_{\text{H-C3-C4}}$ (deg)	121.35 (11)	121.367 (90)	121.396 (26)	121.361 (37)	121.353	121.335
$\theta_{\text{H-C4-C5}}$ (deg)	122.368 (89)	122.344 (41)	122.357 (19)	122.358 (28)	122.349	122.346
$\theta_{\text{C3-C4-C5}}$ (deg)	116.849 (60)	116.849 (16)	116.847 (12)	116.849 (17)	116.847	116.838
$\theta_{\text{N2-C3-C4}}$ (deg)	123.863 (78)	123.860 (23)	123.868 (21)	123.867 (32)	123.879	123.857
$\theta_{\text{N1-N2-C3}}$ (deg)		119.290 (16) ^c	119.285 (17) ^c	119.284 (27) ^c	119.275	119.305
N_{iso}	14	6	17	18		

^aData are given to one additional digit relative to the presentation in ref 5, and the uncertainties here are 2σ rather than 1σ . ^bObtained by applying corrections for the BTE [$\Delta R(\text{best})$] to the CCSD(T)/cc-pCVSZ computed values. ^cValue and uncertainty for additional parameters determined from the r_e^{SE} structure using the alternate Z-matrix described in the Supporting Information.

corrections⁵ reduced the magnitude of the inertial defects for all isotopologues by a factor of 3 and by an additional factor of 10 after the inclusion of electron-mass corrections (Table 2). Though the magnitude of the electron-mass corrections to the rotational constants is small compared to that of the vibration–rotation corrections, the impact of including the electron-mass corrections is clearly significant. Despite the larger numbers of transitions for some isotopologues in the current study, the uncorrected inertial defect ($\Delta_{i,0}$) values are quite similar to those obtained previously. In this work, CCSD(T)/cc-pCVTZ corrections have been applied to the rotational constants, resulting in superior equilibrium inertial defect ($\Delta_{i,e}$) values. There is a larger reduction of the inertial defects from the CCSD(T)/cc-pCVTZ vibration–rotation interaction corrections than from those using an ANO0 basis set. In both cases, however, these are over-corrections that result in negative inertial defect values. The magnitude of the electron-mass corrections is smaller at the CCSD(T)/cc-

pCVTZ level than with the ANO0 basis set. Previously, the same value for the electron-mass correction was applied to every isotopologue, rather than the isotopologue-specific electron-mass corrections used in the current work. As a result, not only are the fully corrected $\Delta_{i,e}$ values obtained using the cc-pCVTZ basis approximately half the magnitude of those obtained using the ANO0 basis (average values -0.00108 vs $0.00207 \mu\text{Å}^2$, respectively), but they also exhibit a considerably smaller standard deviation (0.00014 vs 0.00104 , respectively) (Table 2). The small $\Delta_{i,e}$ values are consistent with the high quality of the spectroscopic constants from the least-squares fits of the rotational spectra and the theoretical corrections employed in this work. These values are quite similar to those determined for pyrimidine¹⁷ using corrections at the same level of theory: $\Delta_{i,e} = 0.01353 \pm 0.00013$ without electron-mass corrections and $\Delta_{i,e} = 0.00151 \pm 0.00013$ with electron-mass corrections. Given the systematic similarities in $\Delta_{i,e}$ between analogous species pyridazine and pyrimidine,¹⁷ or

as previously noted between thiophene¹⁸ and thiazole,¹⁹ it is likely that the inertial defects could be further corrected, despite the sophisticated treatments already employed. Such an improved correction of these inertial defects may be possible through the use of a higher level of theory or basis set to perform the VPT2 or magnetic property calculations, or through use of higher-order vibrational perturbation theory to obtain additional vibration–rotation interaction corrections.

Improvement in the Precision and Accuracy of the Structure. As demonstrated in Table 3, and displayed in Figure 5a, the r_e^{SE} structure of pyridazine determined in this work exhibits structural parameters for which the statistical uncertainties have been reduced by a factor of 2–3 compared to the previous study. Despite the greater precision of the current work, all of the previously determined structural parameters⁵ fall within the 2σ statistical uncertainties of the improved parameters in this work. For all explicitly determined parameters, that is, excluding R_{N1-N2} and $\theta_{N1-N2-C3}$, the statistical uncertainty is less than 0.001 Å for bond lengths and 0.04° for angles. These uncertainties are comparable to those observed in the r_e^{SE} of pyrimidine,²³ whose bond lengths were slightly better determined with all statistical uncertainties (2σ) less than 0.0006 Å. For pyridazine, the r_e^{SE} statistical uncertainties in the C–H distances, ± 0.00023 and ± 0.00024 Å, are three times smaller than the statistical uncertainties in the C–C and C–N distances, $\pm(0.00075-0.00095)$ Å. This was not the case for pyrimidine, in which the statistical uncertainties in C–H distances, $\pm(0.00030-0.00039)$ Å, were only slightly smaller than the statistical uncertainties in C–C and C–N distances, $\pm(0.00038-0.00052)$ Å. These differences in the uncertainties in C–H distances between pyridazine and pyrimidine may arise from symmetry considerations. Pyridazine (C_{2v}) possesses two independent C–H bonds with H-atom positions determined by virtue of ²H-isotopic substitution in 14 of the 18 isotopologues. Pyrimidine possesses three independent C–H bonds with H-atom positions determined by a smaller data set that includes ²H-atom substitution in 11 of 14 isotopologues. Figure 5b presents the number of isotopologues with substitution(s) at the designated position used in the least-squares fit of the structure from all 18 isotopologues. For example, 2 at the C3 position indicates that its substitution is present in two isotopologues: [3-¹³C] and [4-²H, 2-¹³C].²⁰ Symmetric atoms

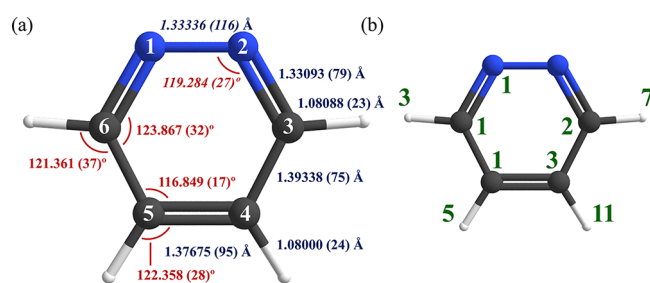


Figure 5. (a) Semi-experimental equilibrium structure (r_e^{SE}) of pyridazine with 2σ uncertainties from least-squares fitting of the isotopologue moments of inertia. The values and uncertainties for R_{N1-N2} and $\theta_{N1-N2-C3}$ (in italic) were determined from the r_e^{SE} structure using the alternate Z-matrix described in the Supporting Information. (b) Number of isotopologues with a substitution relative to the main isotopologue ($o-C_4H_4N_2$) at the labeled atom.

are accounted for separately, as some isotopologues break the C_{2v} symmetry of the parent species.

Quantifying the Importance of Including More Isotopologues in Structure Determinations. To examine the impact on the r_e^{SE} structure of including isotopologues beyond the minimal set necessary to obtain a substitution structure, we obtained an r_e^{SE} structure using only the normal isotopologue and all single isotopic substitutions, which we refer to as “minimal r_e^{SE} ”. As shown in Table 3, the parameter values and uncertainties of the minimal r_e^{SE} agree well with those of the full r_e^{SE} structure. In fact, the uncertainties of the minimal r_e^{SE} are slightly smaller for most of the parameters. The exceptions ($\theta_{H-C3-C4}$ and $\theta_{H-C4-C5}$) are notable, as these are the angles involving a hydrogen atom. The better determination of these angles in the full r_e^{SE} structure is likely due to the inclusion of many more deuterium-substituted isotopologues, relative to the minimal r_e^{SE} set, which includes only two deuterium-substituted isotopologues. Thus, it appears that bond lengths and angles involving only heavy atoms, as well as bond lengths involving hydrogen, are well determined using a minimal set of isotopologues but angles involving hydrogen are not. This conclusion is supported by the behavior of the parameters in the *xrefiteration* analysis (*vide infra*).

The inclusion of additional isotopologues beyond the “minimal set” does indeed improve the overall relative statistical uncertainty of the resulting r_e^{SE} structure. To explore the impact of additional isotopologues on the uncertainty and magnitude of each parameter, we conducted the *xrefiteration* analysis described above. The δr_e^{SE} results of *xrefiteration* are plotted in Figure 6, showing a dramatic decrease in the relative

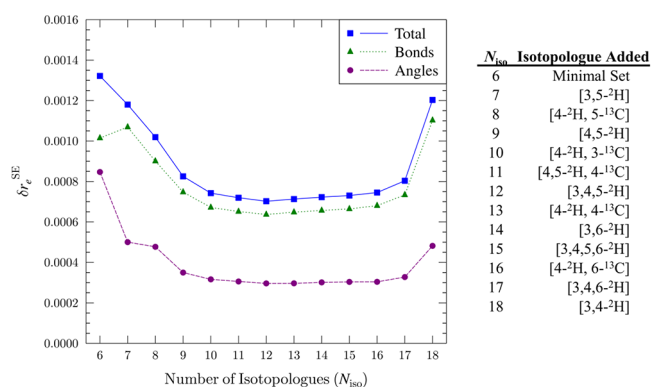


Figure 6. Plot of δr_e^{SE} as a function of the number of isotopologues (N_{iso}) incorporated into the structure determination data set. The total relative statistical uncertainty (δr_e^{SE} , blue squares), the relative statistical uncertainty in the bond distances (green triangles), and the relative statistical uncertainty in the angles (purple circles) are presented.

statistical uncertainty by nearly 50% as the initial isotopologues are added to the r_e^{SE} data set. Such behavior is expected based upon the *xrefiteration* results of pyrimidine,¹⁷ thiophene,¹⁸ thiazole,¹⁹ and hydrazoic acid⁴¹ (*vide infra*). The significant reduction in uncertainty appears to be reversed with the addition of isotopologues in the range of $N_{iso} = 12-18$. There is a slight increase in the uncertainty upon including isotopologues in the range of $N_{iso} = 12-17$, without any discernable pattern in the isotopic substitution or the number of transitions (Table S1) in the least-squares fits for those isotopologues. Thus, we do not suspect that there is an issue with the experimentally determined spectroscopic constants.

The incorporation of [3,4-²H]-pyridazine ($N_{\text{iso}} = 18$), however, results in a dramatic increase in δr_e^{SE} to 0.001204, which is only slightly lower than the value for the minimal r_e^{SE} . From this behavior, we conclude that the structural information provided by [3,4-²H]-pyridazine to the r_e^{SE} is in contradiction with the information provided collectively by the other isotopologues. We can infer, based on the *xrefiteration* algorithm, that at every step of the analysis, the addition of the [3,4-²H] isotopologue resulted in a larger δr_e^{SE} than another isotopologue, so the [3,4-²H] isotopologue was not incorporated into the expanding data set. At the end of the *xrefiteration* analysis, when there were no other isotopologues left, the [3,4-²H] isotopologue was allowed into the structure determination data set.

In the course of this work and other structure determination analyses,^{18,19,41} we observed that similar dramatic increases in the relative statistical uncertainties resulted from a variety of factors, including problems in the fitting of the spectroscopic constants, problems in the rotational constant corrections, or some other problem in the implementation. Such issues appear to be absent in our implementation of the current analysis. For the [3,4-²H] isotopologue in particular, the least-squares fit of the rotational spectrum has low uncertainty ($\sigma_{\text{fit}} = 34$ kHz) with sufficient line count ($N_{\text{lines}} = 619$), and all spectroscopic constants are in reasonable agreement with computational predictions. Furthermore, the corrected inertial defect for this isotopologue ($\Delta_i = -0.00134 \mu\text{Å}^2$) is comparable to those of the other isotopologues, albeit larger than those of all but two isotopologues ([3,5-²H]- and [3,4,6-²H]-pyridazine). Taken collectively, this evidence suggests that the experimental data are accurate and reasonably treated by the vibration–rotation interaction and electron-mass corrections. Thus, we are confident that the behavior of relative statistical uncertainty of the r_e^{SE} upon addition of the [3,4-²H] isotopologue is not due to an issue in data analysis. To better understand the *xrefiteration* plot of pyridazine and the behavior associated with the [3,4-²H] isotopologue, we compared the δr_e^{SE} trends of other molecules (pyrimidine,¹⁷ thiophene,¹⁸ thiazole,¹⁹ and hydrazoic acid⁴¹) to that of pyridazine in Figure 7. The δr_e^{SE} for all five molecules generally decreases as N_{iso} increases. The decrease in δr_e^{SE} is especially pronounced for the first isotopologue addition beyond that minimal set of single isotopic substitutions. As additional isotopologues are incorporated into the data set, δr_e^{SE} continues to decrease for hydrazoic acid, thiophene, and thiazole, until a slight uptick at the end for thiophene and thiazole. Pyridazine and pyrimidine, however, plateau shortly after the initial sharp decrease, then continue to rise slightly through the rest of the *xrefiteration* analysis. In this progression, pyrimidine increases more than pyridazine, until the addition of the final isotopologue to the pyridazine data set. It is clear that the influence of the [3,4-²H]-pyridazine on the r_e^{SE} structure is anomalous in relation to the other isotopologues in this limited set of comparison molecules. Even with the increase in the δr_e^{SE} for pyridazine from $N_{\text{iso}} = 12$ –18, however, the range of δr_e^{SE} values for pyridazine is similar to that of the other structures. Therefore, the increase in the δr_e^{SE} of pyridazine—particularly due to the inclusion of the [3,4-²H] isotopologue—does not necessarily indicate that the r_e^{SE} is not sufficiently determined.

To further assess the quality of the r_e^{SE} and whether the structural parameters are reliable despite the aforementioned behavior of the [3,4-²H]-pyridazine, we examined how the r_e^{SE} parameters change as additional isotopologues are included

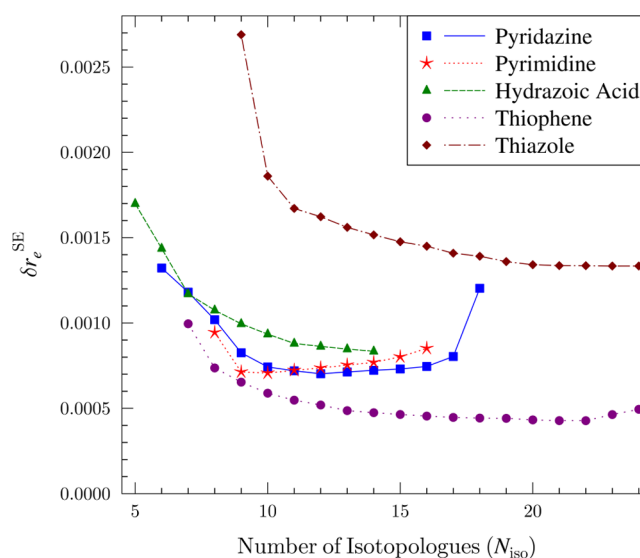


Figure 7. Comparison of total relative statistical uncertainty (δr_e^{SE}) as additional isotopologues are included in the data set for the r_e^{SE} structure determination of hydrazoic acid,⁴¹ pyrimidine,¹⁷ pyridazine, thiophene,¹⁸ and thiazole,¹⁹ beginning from each of their respective minimal set of isotopologues.

(Figure 8). Interestingly, the value of the $\theta_{\text{H-C3-C4}}$ angle in the final iteration ($N_{\text{iso}} = 18$) is closer to its value in the minimal set ($N_{\text{iso}} = 6$) than the intermediate iterations, which determine a larger angle. Given our confidence in the data of the [3,4-²H] isotopologue, the trend in the $\theta_{\text{H-C3-C4}}$ angle suggests that the other isotopologues added to the minimal set are quite consistent with respect to their impact on this angle, while also not providing new or sufficient information for determining this angle. This interpretation is further supported by comparison to the BTE value, which shows that the intermediate isotopologues cause the angle to deviate away from the BTE value. Examination of the other parameters reveals that $R_{\text{C4-C5}}$, $R_{\text{C3-C4}}$, and $R_{\text{N2-C3}}$ have similar, though less pronounced, behavior. The inclusion of the last few isotopologues, especially the [3,4-²H] isotopologue, brings the parameters into a better agreement with the theoretical prediction because these isotopologues are providing structural information that is not contained in the preceding iterations of the data set.

The C3 atom, which lies very close to the *b*-axis, is present in three of the four parameters whose values deviate away from the BTE. The difficulty in determining the C3 atom position was described in the original r_s structure determination¹⁵ and seemingly addressed in the subsequent r_s and first r_e^{SE} structure determination by greater isotopic substitution.⁵ Based upon this analysis, however, it appears that the classical difficulty in determining the position of atoms that lie close to an inertial axis by Kraitchman analysis^{21,22} may not be fully addressed even with the first 17 isotopologues in this work. The inclusion of the [3,4-²H] isotopologue has a profound effect on the $\theta_{\text{H-C3-C4}}$ angle. The simultaneous isotopic substitution of the hydrogen atoms at C3 and C4 causes a significant rotation of the principal axes (Table S4) such that C3 (and the symmetric C6) are no longer close to the *b*-axis. It should be noted that other isotopologues have rotations of similar magnitude. Finally, the two hydrogen-containing angles have considerable improvement in the uncertainties and the greatest change to their values when isotopologues beyond the minimal set are

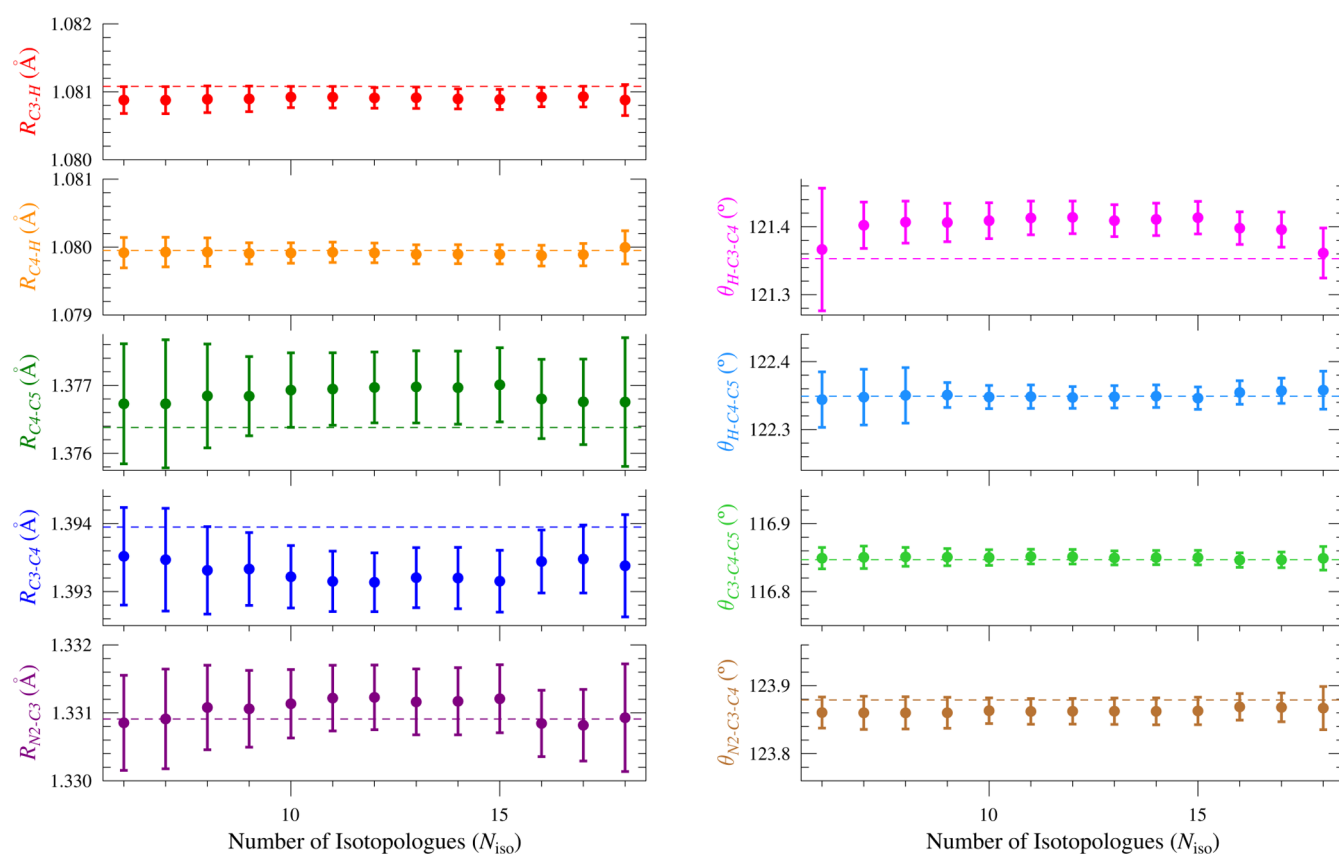


Figure 8. Plots of structural parameters as a function of the number of isotopologues (N_{iso}) and their 2σ uncertainties, with consistent scales for each distance (0.002 Å) and each angle (0.2°). The dashed line in each plot is the BTE value calculated for that parameter. The isotopologue ordering along the x -axis is the same as that in Figure 6.

included. Such behavior suggests that the minimal set of single-substitution isotopologues is not sufficient for a precise determination of these angles and that the improvement in the uncertainties in the full r_e^{SE} structure for these angles is partly due to the increased number of isotopologues.

Best Theoretical Estimate. As in the structure determination of pyrimidine,¹⁷ all structural parameters of the BTE of pyridazine fall within the 2σ uncertainties of their corresponding parameters for the r_e^{SE} structure of pyridazine (Figure 9 and Table 3). Impressively, five of the nine independent BTE structural parameters fall within the 1σ statistical uncertainties of the r_e^{SE} parameters in this work, which is reasonably close to the statistical expectation for a normal distribution. As can be seen from Table 3, all of the r_e^{SE} bond angles fall within 0.01 degrees of the corresponding BTE values. The agreement is largely due to the quintuple-zeta basis set since all of the CCSD(T)/cc-pCVSZ structural parameters are also within the 2σ uncertainties of the corresponding r_e^{SE} parameters. Indeed, examination of the CCSD(T)/cc-pCVQZ structural parameters (Table S5) reveals that only four of the nine independent parameters resulting from the smaller basis agree with the r_e^{SE} structure. The difference between the quadruple-zeta and quintuple-zeta calculations, however, is only noticeable because of the small uncertainties in the current r_e^{SE} structure of pyridazine. All parameters of the CCSD(T)/cc-pCVQZ r_e fell within 2σ of all the previously determined r_e^{SE} parameters,⁵ due to the larger statistical uncertainties in that work.

Examination of the individual corrections included in the BTE in Table 4 reveals differences in the effects of the various corrections for bond distances. The ΔR (basis) and Δ (rel)

corrections shorten the bond distances from those predicted at the quintuple-zeta basis set, while the ΔR (corr) correction lengthens them. Overall, the corrections lead to a partial cancellation that brings the BTE r_e structure into better agreement with the r_e^{SE} structure.

CONCLUSIONS

We determined a highly accurate and precise semi-experimental structure (r_e^{SE}) for pyridazine with statistical uncertainties of <0.001 Å and $<0.04^\circ$ (2σ) for the bond distances and angles, respectively, and in complete agreement with the BTE. The improvement in the r_e^{SE} structure in this work is largely due to improved theoretical corrections. Our iterative analysis of the r_e^{SE} structure determination (*xrefiteration*) as a function of additional isotopologues beyond the minimal set can be utilized to examine not only the improvement in the r_e^{SE} determination as additional isotopologues are added, but also the relationship between an individual isotopologue and the rest of the data set. The *xrefiteration* plots can be especially useful for identifying outliers that occur due to problems in the spectroscopic analysis or the implementation of the r_e^{SE} structure determination. When the spectroscopic constants are reliable and the structure determination is implemented correctly, the *xrefiteration* plots reveal important trends in how the individual parameters vary as a function of the number of isotopologues. This provides insights into the structural information contributed by individual isotopologues. Finally, the *xrefiteration* plots can reveal which r_e^{SE} parameters are well-converged

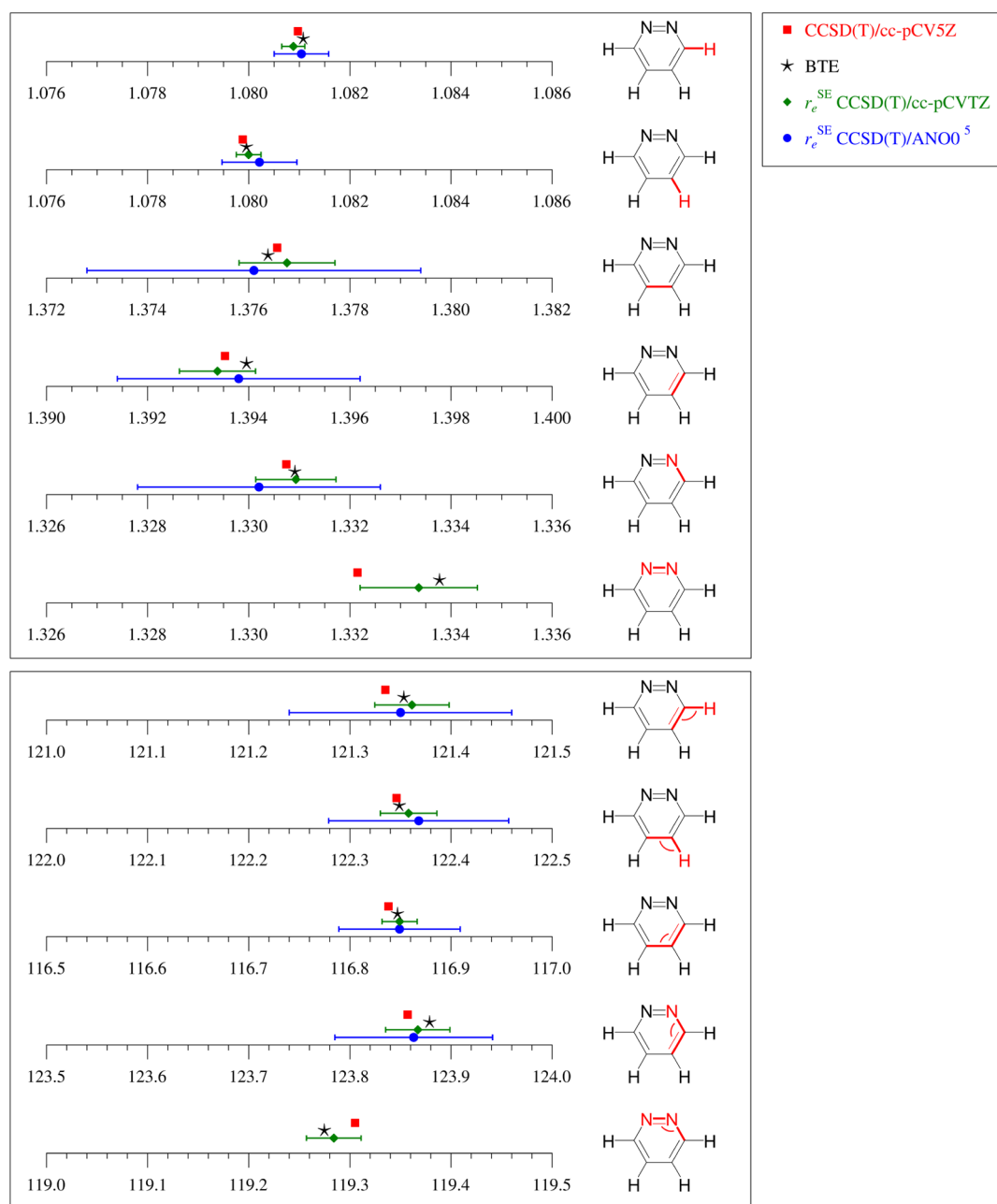


Figure 9. Graphical comparison of pyridazine structural parameters with bond distances in angstroms (Å) and angles in degrees (°). Uncertainties shown are 2σ . Data for r_e^{SE} CCSD(T)/ANO0 are taken from ref 5. The values and uncertainties for $R_{\text{N1-N2}}$ (top box, last row) and $\theta_{\text{N1-N2-C3}}$ (bottom box, last row) were determined from the r_e^{SE} structure using the alternate Z-matrix described in the Supporting Information.

Table 4. Corrections (ΔR) Used for Obtaining the Best Theoretical Estimate (BTE)

parameter	ΔR (basis) eq 1	ΔR (corr) eq 2	ΔR (rel) eq 3	ΔR (DBOC) eq 4	ΔR (best) eq 5
$R_{\text{C3-H}}$ (Å)	-0.000040	0.00012	-0.00011	0.00014	0.00011
$R_{\text{C4-H}}$ (Å)	-0.000063	0.00012	-0.00011	0.00014	0.000074
$R_{\text{C4-C5}}$ (Å)	-0.00034	0.00042	-0.00024	-0.00022	-0.00018
$R_{\text{C3-C4}}$ (Å)	-0.00021	0.00080	-0.00023	0.000058	0.00042
$R_{\text{N2-C3}}$ (Å)	-0.00014	0.00042	-0.000089	-0.00022	0.00017
$\theta_{\text{H-C3-C4}}$ (deg)	0.032	-0.019	0.0030	0.0023	0.018
$\theta_{\text{H-C4-C5}}$ (deg)	-0.00085	0.0026	0.0011	0.000045	0.0028
$\theta_{\text{C3-C4-C5}}$ (deg)	0.010	-0.00083	-0.00045	0.00065	0.0090
$\theta_{\text{N2-C3-C4}}$ (deg)	-0.020	0.029	0.014	-0.0012	0.022

and which may benefit from the incorporation of additional isotopologues.

We are confident that the behavior of the $[3,4\text{-}^2\text{H}]$ isotopologue in the *xrefiteration* analysis is a real phenomenon

and not a manifestation of a problem in the analysis or implementation. Given the impressive agreement between the BTE and the r_e^{SE} parameters, we can examine how this agreement is affected by the presence or absence of the $[3,4\text{-}^2\text{H}]$ isotopologue. When the $[3,4\text{-}^2\text{H}]$ isotopologue is excluded from the data set, the resulting r_e^{SE} does not display good agreement with the BTE (Table 3) for the two hydrogen-containing bond angles, $\theta_{\text{H-C3-C4}}$ and $\theta_{\text{H-C4-C5}}$. The better agreement between the r_e^{SE} structure and the BTE when $[3,4\text{-}^2\text{H}]$ is included indicates that the apparent improvement in statistical uncertainty as the other isotopologues were added to the minimal set (Figure 6) is actually deceptive; the preceding data sets did not include the isotopologue that is important for determining $\theta_{\text{H-C3-C4}}$ and $\theta_{\text{H-C4-C5}}$. If the r_e^{SE} structure remains stable as additional isotopologues are incorporated beyond the 18 utilized in this work, it would confirm the validity of this assertion. New syntheses—beyond the scope of this work—would be required, as all possible isotopologues observable in commercial pyridazine or in the deuterated samples used in the previous and current works are included in the current r_e^{SE} . While it is not a member of the canonical set of singly-substituted isotopologues, the $[3,4\text{-}^2\text{H}]$ isomer appears to be vital in structure determination, as this substitution tends to rotate the principal axes in such a way that the C3 and C6 atoms are pulled away from the b -axis. The standard problem in structure determination that is posed by near-axis atoms is lessened for this isotopomer, and an improved determination follows. Regardless of the reason, the impact of the $[3,4\text{-}^2\text{H}]$ on the structure determination is as significant as it is unexpected, serving to reinforce the notion that structure determinations should seek to incorporate a variety of isotopologues to ensure that the atom positions can be satisfactorily determined.

The agreement of the r_e^{SE} and BTE structures is impressive. What was unexpected, to us, is the finding that the minimal set of six isotopologues provided r_e^{SE} structural parameters that are equally accurate and precise as those determined using the much larger set of 18 isotopologues. This case stands in sharp contrast to our findings for similar structure determinations of pyrimidine,¹⁷ thiophene,¹⁸ and thiazole.¹⁹ At the current time, it is not understood, *a priori*, whether a particular structure will be accurately determined from the minimal set of isotopologues. The unexpected significance of the $[3,4\text{-}^2\text{H}]$ -isotopologue in the structure determination of pyridazine suggests that the best practice remains to include as many isotopologues as is practical.

■ ASSOCIATED CONTENT

Supporting Information

The Supporting Information is available free of charge at <https://pubs.acs.org/doi/10.1021/acs.jpca.1c06187>.

Directories of spectral fit files, tables of spectroscopic constants, data distribution plots, directories of computational output files, description of the alternate Z -matrix, results of *xrefiteration* analysis, and a detailed explanation and usage guide of the *xrefiteration* script (PDF)

ASFIT data files, CFOUR optimizations and anharmonic frequency outputs, *xrefit* outputs, and the *xrefiteration* script and associated files (ZIP)

■ AUTHOR INFORMATION

Corresponding Authors

R. Claude Woods – Department of Chemistry, University of Wisconsin-Madison, Madison, Wisconsin 53706, United States; orcid.org/0000-0003-0865-4693;
Email: rcwoods@wisc.edu

Robert J. McMahon – Department of Chemistry, University of Wisconsin-Madison, Madison, Wisconsin 53706, United States; orcid.org/0000-0003-1377-5107;
Email: robert.mcmahon@wisc.edu

Authors

Andrew N. Owen – Department of Chemistry, University of Wisconsin-Madison, Madison, Wisconsin 53706, United States

Maria A. Zdanovskaia – Department of Chemistry, University of Wisconsin-Madison, Madison, Wisconsin 53706, United States; orcid.org/0000-0001-5167-8573

Brian J. Esselman – Department of Chemistry, University of Wisconsin-Madison, Madison, Wisconsin 53706, United States; orcid.org/0000-0002-9385-8078

John F. Stanton – Quantum Theory Project, Departments of Physics and Chemistry, University of Florida, Gainesville, Florida 32611, United States

Complete contact information is available at:
<https://pubs.acs.org/10.1021/acs.jpca.1c06187>

Notes

The authors declare no competing financial interest.

■ ACKNOWLEDGMENTS

We gratefully acknowledge the National Science Foundation for support of this project (R.J.M. CHE-1664912, CHE-1954270, and J.F.S. CHE-1664325). We thank Michael McCarthy for the loan of an amplification-multiplication chain and the Harvey Spangler Award (to B.J.E.) for funding that supported purchase of the corresponding detector.

■ REFERENCES

- (1) Dey, S.; Manogaran, D.; Manogaran, S.; Schaefer, H. F. Quantification of Aromaticity of Heterocyclic Systems Using Interaction Coordinates. *J. Phys. Chem. A* **2018**, *122*, 6953–6960.
- (2) Levandowski, B. J.; Abularrage, N. S.; Raines, R. T. Differential Effects of Nitrogen Substitution in 5- and 6-Membered Aromatic Motifs. *Chem. Eur. J.* **2020**, *26*, 8862–8866.
- (3) Simon, M. N.; Simon, M. Search for Interstellar Acrylonitrile, Pyrimidine, and Pyridine. *Astrophys. J.* **1973**, *184*, 757.
- (4) Charnley, S. B.; Kuan, Y.-J.; Huang, H.-C.; Botta, O.; Butner, H. M.; Cox, N.; Despois, D.; Ehrenfreund, P.; Kisiel, Z.; Lee, Y.-Y.; et al. Astronomical searches for nitrogen heterocycles. *Adv. Space Res.* **2005**, *36*, 137–145.
- (5) Esselman, B. J.; Amberger, B. K.; Shutter, J. D.; Daane, M. A.; Stanton, J. F.; Woods, R. C.; McMahon, R. J. Rotational Spectroscopy of Pyridazine and its Isotopologs from 235–360 GHz: Equilibrium Structure and Vibrational Satellites. *J. Chem. Phys.* **2013**, *139*, 224304.
- (6) Cernicharo, J.; Heras, A. M.; Tielens, A. G. G. M.; Pardo, J. R.; Herpin, F.; Guélin, M.; Waters, L. B. F. M. Infrared Space Observatory's Discovery of C_4H_2 , C_6H_2 , and Benzene in CRL 618. *Astrophys. J.* **2001**, *546*, L123–L126.
- (7) McMahon, R. J.; McCarthy, M. C.; Gottlieb, C. A.; Dudek, J. B.; Stanton, J. F.; Thaddeus, P. The Radio Spectrum of the Phenyl Radical. *Astrophys. J.* **2003**, *590*, L61–L64.
- (8) Lovas, F. J.; McMahon, R. J.; Grabow, J.-U.; Schnell, M.; Mack, J.; Scott, L. T.; Kuczkowski, R. L. Interstellar Chemistry: A Strategy

for Detecting Polycyclic Aromatic Hydrocarbons in Space. *J. Am. Chem. Soc.* **2005**, *127*, 4345–4349.

(9) Widicus Weaver, S. L.; Remijan, A. J.; McMahon, R. J.; McCall, B. J. A Search for *ortho*-Benzyne (*o*-C₆H₄) in CRL 618. *Astrophys. J.* **2007**, *671*, L153–L156.

(10) Zdanovskaia, M. A.; Esselman, B. J.; Woods, R. C.; McMahon, R. J. The 130 - 370 GHz Rotational Spectrum of Phenyl Isocyanide (C₆H₅NC). *J. Chem. Phys.* **2019**, *151*, 024301.

(11) Dorman, P. M.; Esselman, B. J.; Park, J. E.; Woods, R. C.; McMahon, R. J. Millimeter-wave spectrum of 4-cyanopyridine in its ground state and lowest-energy vibrationally excited states, ν_{20} and ν_{30} . *J. Mol. Spectrosc.* **2020**, *369*, 111274.

(12) Dorman, P. M.; Esselman, B. J.; Woods, R. C.; McMahon, R. J. An analysis of the rotational ground state and lowest-energy vibrationally excited dyad of 3-cyanopyridine: Low symmetry reveals rich complexity of perturbations, couplings, and interstate transitions. *J. Mol. Spectrosc.* **2020**, *373*, 111373.

(13) McGuire, B. A.; Burkhardt, A. M.; Kalenskii, S.; Shingledecker, C. N.; Remijan, A. J.; Herbst, E.; McCarthy, M. C. Detection of the aromatic molecule benzonitrile (C₆H₅CN) in the interstellar medium. *Science* **2018**, *359*, 202–205.

(14) McGuire, B. A.; Loomis, R. A.; Burkhardt, A. M.; Lee, K. L. K.; Shingledecker, C. N.; Charnley, S. B.; Cooke, I. R.; Cordiner, M. A.; Herbst, E.; Kalenskii, S.; et al. Detection of two interstellar polycyclic aromatic hydrocarbons via spectral matched filtering. *Science* **2021**, *371*, 1265–1269.

(15) Werner, W.; Dreizler, H.; Rudolph, H. D. Zum Mikrowellenspektrum Des Pyridazins. *Z. Naturforsch., A: Phys. Sci.* **1967**, *22*, 531–543.

(16) López, J. C.; de Luis, A.; Blanco, S.; Lesarri, A.; Alonso, J. L. Investigation of the quadrupole coupling hyperfine structure due to two nuclei by molecular beam Fourier transform microwave spectroscopy: spectra of dichlorofluoromethane and pyridazine. *J. Mol. Struct.* **2002**, *612*, 287–303.

(17) Heim, Z. N.; Amberger, B. K.; Esselman, B. J.; Stanton, J. F.; Woods, R. C.; McMahon, R. J. Molecular structure determination: Equilibrium structure of pyrimidine (*m*-C₄H₄N₂) from rotational spectroscopy (r_e^{SE}) and high-level ab initio calculation (r_e) agree within the uncertainty of experimental measurement. *J. Chem. Phys.* **2020**, *152*, 104303.

(18) Orr, V. L.; Ichikawa, Y.; Patel, A. R.; Kougias, S. M.; Kobayashi, K.; Stanton, J. F.; Esselman, B. J.; Woods, R. C.; McMahon, R. J. Precise Equilibrium Structure Determination of Thiophene (*c*-C₄H₄S) by Rotational Spectroscopy – Structure of a Five-Membered Heterocycle Containing a Third-Row Atom. *J. Chem. Phys.* **2021**, *154*, 244310.

(19) Esselman, B. J.; Zdanovskaia, M. A.; Owen, A. N.; Stanton, J. F.; Woods, R. C.; McMahon, R. J. Precise Equilibrium Structure of Thiazole (*c*-C₃H₃NS) from Twenty-Four Isotopologues. *J. Chem. Phys.* **2021**, *155*, 054302.

(20) The proper numbering for the isotopologue that we designate as [4-²H, 6-¹³C] is actually [5-²H, 3-¹³C]. The latter numbering scheme, however, obscures the relationship with the other 4-²H substituted isotopologues.

(21) Kraitchman, J. Determination of Molecular Structure from Microwave Spectroscopic Data. *Am. J. Phys.* **1953**, *21*, 17–24.

(22) Costain, C. C. Determination of Molecular Structures from Ground State Rotational Constants. *J. Chem. Phys.* **1958**, *29*, 864–874.

(23) Amberger, B. K.; Esselman, B. J.; Stanton, J. F.; Woods, R. C.; McMahon, R. J. Precise Equilibrium Structure Determination of Hydrazoic Acid (HN₃) by Millimeter-wave Spectroscopy. *J. Chem. Phys.* **2015**, *143*, 104310.

(24) Kisiel, Z.; Pszczółkowski, L.; Drouin, B. J.; Brauer, C. S.; Yu, S.; Pearson, J. C.; Medvedev, I. R.; Fortman, S.; Neese, C. Broadband rotational spectroscopy of acrylonitrile: Vibrational energies from perturbations. *J. Mol. Spectrosc.* **2012**, *280*, 134–144.

(25) Kisiel, Z.; Pszczółkowski, L.; Medvedev, I. R.; Winnewisser, M.; De Lucia, F. C.; Herbst, E. Rotational spectrum of *trans*–*trans* diethyl

ether in the ground and three excited vibrational states. *J. Mol. Spectrosc.* **2005**, *233*, 231–243.

(26) Kisiel, Z. Assignment and Analysis of Complex Rotational Spectra. In *Spectroscopy from Space*; Demaison, J., Sarka, K., Cohen, E. A., Eds.; Kluwer Academic Publishers: Dordrecht, 2001; pp 91–106. <http://www.ifpan.edu.pl/~kisiel/prospe.htm>.

(27) Stanton, J. F.; Gauss, J.; Cheng, L.; Harding, M. E.; Matthews, D. A.; Szalay, P. G. *CFOUR*, a quantum chemical program package, with contributions from A. A. Auer, R. J. Bartlett, U. Benedikt, C. Berger, D. E. Bernholdt, Y. J. Bomble, O. Christiansen, F. Engel, R. Faber, M. Heckert, O. Heun, C. Huber, T.-C. Jagau, D. Jonsson, J. Jusélius, K. Klein, W. J. Lauderdale, F. Lipparini, T. Metzroth, L. A. Mück, D. P. O'Neill, D. R. Price, E. Prochnow, C. Puzzarini, K. Ruud, F. Schiffmann, W. Schwalbach, C. Simmons, S. Stopkiewicz, A. Tajti, J. Vázquez, F. Wang, J. D. Watts and the integral packages MOLECULE (J. Almlöf and P. R. Taylor), PROPS (P. R. Taylor), ABACUS (T. Helgaker, H. J. Aa. Jensen, P. Jørgensen, and J. Olsen), and ECP routines by A. V. Mitin and C. van Wüllen. For the current version, see <http://www.cfour.de>.

(28) Peterson, K. A.; Kendall, R. A.; Dunning, T. H. Benchmark Calculations with Correlated Molecular Wave-Functions .2. Configuration-Interaction Calculations on 1st-Row Diatomic Hydrides. *J. Chem. Phys.* **1993**, *99*, 1930–1944.

(29) Woon, D. E.; Dunning, T. H., Jr. Benchmark calculations with correlated molecular wave functions .VI. Second row A₂ and first row/second row AB diatomic molecules. *J. Chem. Phys.* **1994**, *101*, 8877–8893.

(30) Bomble, Y. J.; Stanton, J. F.; Kállay, M.; Gauss, J. Coupled-cluster methods including noniterative corrections for quadruple excitations. *J. Chem. Phys.* **2005**, *123*, 054101.

(31) Dyall, K. G. Interfacing relativistic and nonrelativistic methods. IV. One- and two-electron scalar approximations. *J. Chem. Phys.* **2001**, *115*, 9136–9143.

(32) Liu, W.; Peng, D. Exact two-component Hamiltonians revisited. *J. Chem. Phys.* **2009**, *131*, 031104.

(33) Cheng, L.; Gauss, J. Analytic energy gradients for the spin-free exact two-component theory using an exact block diagonalization for the one-electron Dirac Hamiltonian. *J. Chem. Phys.* **2011**, *135*, 084114.

(34) Born, M.; Huang, K. *Dynamical Theory of Crystal Lattices*; Oxford University Press: New York, 1956.

(35) Handy, N. C.; Yamaguchi, Y.; Schaefer, H. F., III The Diagonal Correction to the Born-Oppenheimer Approximation: Its Effect on the Singlet-Triplet Splitting of CH₂ and Other Molecular Effects. *J. Chem. Phys.* **1986**, *84*, 4481–4484.

(36) Gordy, W.; Cook, R. *Microwave Molecular Spectra*, 3rd ed.; Wiley Interscience: New York, 1984; Vol. XVIII.

(37) Puzzarini, C.; Bloino, J.; Tasinato, N.; Barone, V. Accuracy and Interpretability: The Devil and the Holy Grail. New Routes across Old Boundaries in Computational Spectroscopy. *Chem. Rev.* **2019**, *119*, 8131–8191.

(38) Demaison, J.; Vogt, N.; Ksenafontov, D. N. Accuracy of semiexperimental equilibrium structures: Sulfine as an example. *J. Mol. Struct.* **2020**, *1206*, 127676.

(39) For an overview of methods used to treat cases for which a sufficient number of isotopologues is not available, see Puzzarini, C.; Barone, V. Diving for Accurate Structures in the Ocean of Molecular Systems with the Help of Spectroscopy and Quantum Chemistry. *Acc. Chem. Res.* **2018**, *51*, 548–556.

(40) For pyridazine in this work, 12 additional isotopologues beyond the core set corresponds to 12! ≈ 479,000,000 permutations and, assuming 0.1 s per *xrefit* execution, ~13,000 processor hours.

(41) Owen, A. N.; Sahoo, N. P.; Esselman, B. J.; Stanton, J. F.; Woods, R. C.; McMahon, R. J. Improved Structure Determination of Hydrazoic Acid (HN₃). Unpublished.